Polymer Testing 98 (2021) 107163

Contents lists available at ScienceDirect

Polymer Testing

journal homepage: http://www.elsevier.com/locate/polytest

Study on the preferential distribution of acetyl tributyl citrate in poly (lactic) acid-poly(butylene adipate-co-terephthalate) blends

Laura Aliotta [a,b], Ilaria Canesi [c], Andrea Lazzeri [a,b,c,*]

[a] University of Pisa, Department of Civil and Industrial Engineering, Via Diotisalvi, 2, 56122, Pisa, Italy
[b] Interuniversity National Consortium of Materials Science and Technology (INSTM), Via Giusti 9, 50121, Florence, Italy
[c] Planet Bioplastics s.r.l., Via San Giovanni Bosco 23, 56127, Pisa, Italy

ARTICLE INFO

Keywords:
Poly(lactic acid) (PLA)
Poly(butylene adipate-co-terephthalate) (PBAT)
Binary blends
Plasticiser
Additives

ABSTRACT

In this work, the preferential distribution of acetyl tributyl citrate plasticiser (ATBC) in poly(lactic acid) (PLA)-poly(butylene adipate-co-terephthalate) PBAT blends has been investigated. Pure plasticised PLA and PBAT blends and their binary blends (PLA/PBAT with 80 wt% of PLA and 20 wt% of PBAT and PBAT/PLA with 80 wt% of PBAT and 20 wt% of PLA) containing different ATBC amount (from 5 to 20 wt%) have been investigated. Dynamic mechanical thermal analysis (DMTA) has been performed in order to evaluate the shift of the glass transition temperature (T_g) in both the polymer systems. The results obtained showed a larger shift for PLA than the PBAT and the calculated plasticiser partition coefficient for both binary blends revealed a preferential distribution of ATBC in the PLA phase rather than PBAT ($K_{A/B} = 1.07$ for PLA-based system and $K_{A/B} = 1.45$ for PBAT-based system). The results obtained have also been confirmed by the Hansen Solubility Parameters (HSPs) methodology. The study is finally augmented by the differential scanning calorimetry (DSC) and morphology analysis in order to demonstrate the possible effects of crystallinity on the plasticiser distribution in the binary blends.

1. Introduction

The growing interest on the development of more environmentally friendly polymeric materials with biodegradable and recyclable properties has laid the basis for the twenty-first-century portfolio for the production of sustainable and eco-efficient plastics [1]. The increasing preoccupation caused by the problems in the disposal of the conventional plastics has pushed the researchers towards the development of new biobased and/or biodegradable materials with adequate properties to be able to respond to the market needs especially in those sectors where the plastic consume is very high such as single-use packaging or horticulture [2–4].

Among all the biodegradable polymers, poly(lactic acid) (PLA), often referred to as poly(L,D-lactide), is the front runner in the emerging bioplastics market thanks to its wide availability, its origin from renewable resources and affordable cost [5]. The PLA compostability coupled with its sustainability makes it a promising material for reducing the societal solid waste disposal problems [6,7]. In addition to its biodegradability and renewability, PLA also exhibits interesting mechanical properties that are on par to those of oil-based and non-biodegradable polymers. In particular, PLA possesses a high stiffness (with a Young's modulus of about 3–4 GPa) and high strength at break (between 50 and 60 MPa) [8,9]. However, PLA often shows some drawbacks depending on the application in which it is used, where it becomes too stiff and brittle (with a poor Charpy notched impact resistance of about 2.5–3 kJ/m^2). Furthermore, PLA has a very slow crystallisation rate and shows poor thermal properties due to its glass transition temperature of around 60 °C [10,11]. A modulation of PLA properties is required depending on its final application; often it is necessary to use a plasticiser or to introduce rubber particles to improve its elongation at break and impact properties [12,13].

The addition of a plasticiser to PLA induces a decrease in its glass transition temperature (T_g) and results in a decrement of its stress at break accompanied by an increment of elongation at break. For films or sheets applications the addition of an optimised amount of plasticiser greatly improves the properties and functionalities [14]. The choice of the appropriate plasticisers, especially for the biobased and/or biodegradable applications, is however limited by the environmental impact and physical-chemical properties, that dictated their miscibility with the polymeric matrix [15]. For this purpose, either glycerol or its ester

* Corresponding author. University of Pisa, Department of Civil and Industrial Engineering, Via Diotisalvi, 2, 56122, Pisa, Italy.
E-mail address: andrea.lazzeri@unipi.it (A. Lazzeri).

https://doi.org/10.1016/j.polymertesting.2021.107163
Received 2 January 2021; Received in revised form 15 February 2021; Accepted 8 March 2021
Available online 20 March 2021

derivatives have been added to PLA and optimised [16,17]. Similarly, significant works have also been done on adding the citrate derivatives (such as tributyl citrate (TBC), acetyl triethyl citrate (TEC) and acetyl tributyl citrate (ATBC)) as plasticisers to PLA systems [18–20]. In particular, TBC and ATBC interact well with PLA improving its crystallisation rate and ductility [20]. On the basis of the literature work, ATBC has been classified as an efficient biobased and biodegradable plasticiser for PLA based systems [21,22]. Labrecque et al. [19] demonstrated that all citrate esters (TEC, ATBC and TBC) reduced efficiently the PLA glass transition temperature and improved the final elongation at break; however, with ATBC the lowest glass transition temperature was registered. Furthermore, Courgneau et al. revealed that the neat poly(L,D-lactide), melt blended with talc and ATBC, is a promising system to promote the crystallisation of PLA and it should efficiently be co-optimised to tailor the final properties of PLA-based systems [23].

In order to increase the PLA ductility, physical blending with a softer biobased and/or biodegradable polymer was investigated as an economical and efficient way to tune the final properties of PLA [24]. Among the biodegradable soft polymers, (derived or not from renewable resource) different attempts were made by blending PLA with poly (caprolactone) (PCL) [25–28], poly(butylene succinate) (PBS) [29–31], poly(butylene succinate-co-adipate) (PBSA) [32–34] and poly(hydroxybutyrate) (PHBs) [35–37]. In particular, the blending of PLA with poly (butylene adipate-co-terephthalate) (PBAT) was intensively studied [12, 38–41]. This system revealed a significant improvement of the PLA ductility and a better processability (with an increased melt processability window [42]). A well dispersed systems constituted by the PBAT particles into the PLA matrix can be obtained by melt blending in a twin screw-extruder up to 20 wt% of PBAT content [12,43,44]. This morphology was ascribed to the high immiscibility existing between the two polymers (they have different Hildebrand solubility parameters [PLA $\approx$ 653.3 $(kJ/m^3)^{1/2}$ and PBAT $\approx$ 1484.48 $(kJ/m^3)^{1/2}$] [45]) and to the poor interfacial adhesion between the two polymeric phases [46].

To better modulate the final mechanical properties of PLA, it is fundamental to understand the relationship between the final mechanical properties, blend composition, compatibility level and the effect of processing on the morphology of the system. Accordingly, in this study, the effect of the plasticiser addition onto the PLA and PBAT binary blend system has been systematically investigated. In particular, the possible preferential distribution of a low molecular weight plasticiser into one polymeric phase rather than the other has been explored. Notably, this work represents a development of the work reported by Coltelli at al [22]. To this purpose, the attention has been focused on the effects of different quantities of ATBC plasticiser that varied from 5 to 20 wt%. In order to better understand the eventual preferential solubilisation of ATBC in the PLA or in the PBAT, a first screening study has been conducted on the two polymeric matrices separately. Then, the effect of ATBC addition has further been investigated on the PLA and PBAT binary blends. Two similar blends have been investigated towards evaluating whether the eventual morphology of the system influences the ATBC preferentiality on the binary blend system comprising of the PLA matrix blend containing 20 wt% of PBAT (PLA/PBAT blends) and a PBAT matrix blend containing 20 wt% of PLA (PBAT/PLA blends).

The 20 wt% of PBAT content in the PLA matrix (and vice versa) was chosen because this blend morphology is far from the phase inversion and/or the co-continuous morphology [12], in addition, the content of dispersed phase is a significant quantity to better investigate the preferentiality of the plasticiser in the two polymers (PLA and PBAT).

Furthermore, the variation in the glass transition temperature (T_g) due to the addition of plasticiser has been evaluated by dynamic mechanical thermal analysis (DMTA), which provided the T_g lowering with good accuracy. From the obtained DMTA results, the partition coefficient (*K)* has been calculated by adopting the method proposed by Sperling at al. [47], which is typically used to evaluate the partitioning of plasticisers in the two-phase systems. The results have also been compared with the estimation of the ATBC affinity with PLA and PBAT carried out by the Hansen Solubility Parameters (HSPs) methodology [48,49]. In addition, in order to understand whether the eventual crystallisation phenomenon can also influence the plasticiser distribution and concentration, a differential scanning calorimetry analysis (DSC) has been carried out. This is essentially because of the fact that the plasticiser is located in the amorphous polymeric region and the change in crystalline properties of the systems can influence the distribution of the plasticiser.

The aim of this work is focused on the determination on the preferential distribution of ATBC in PLA/PBAT blends. From this study emerged that ATBC is more akin to PLA than PBAT. This result has also been validated by the marked lowering of the T_g of the PLA, both in the pure matrices and binary systems. Moreover, the samples containing PBAT at high plasticiser content as well as the PBAT/PLA blends showed a remarkable migration of plasticiser after some weeks from the extrusion of the specimens and injection moulding processes (this phenomenon will be further investigated from the kinetics point of view in another work). The chemical compatibility, calculated by the HSPs method, showed a borderline solubility of ATBC within PBAT, which can probably accelerate the kinetics of migration of the plasticiser onto the surface of the specimen. However, the HSPs analysis confirmed the poor affinity between ATBC and PBAT. Finally, the blends morphology and crystallinity do not seem to influence the results obtained which are exclusively linked to the greater affinity of ATBC towards PLA.

2. Theoretical analysis

2.1. Glass transition composition dependence

Several theoretical equations have been formulated to describe the glass transition (T_g) composition dependence of the polymer-polymer and polymer-plasticiser (small molecule) systems. However, it must be pointed out that generally the equation developed for one system may not be applicable to another system [50].

However in particular, the equation developed by Fox [51] (Eq. (1)) is generally adopted to predict the glass transition temperature of a polymer-polymer system:

$$\frac{1}{T_g} = \frac{m_1}{T_{g_1}} + \frac{m_2}{T_{g_2}} \tag{1}$$

where, the T_{g1} and T_{g2} are the glass transition temperatures of the pure components and m_1 and m_2 are their weight fractions, respectively.

On the other hand, for a polymeric system in which a low molecular weight plasticiser is added in a low percentage concentrations [52], a linear decrease of transition temperature with increasing plasticiser content is generally observed [50,53,54]:

$$T_g = T_{gp} - Bm_2 \tag{2}$$

where T_{gp} is the polymer glass transition, m_2 is the weight fraction of the plasticiser and B is a constant typical of the system analysed. This formulation of the T_g equation has been obtained by a number of authors via a variety of approaches such as isofree volume [55], isoviscous [56] and viscous flow [57].

2.2. Calculation of the plasticiser partition coefficient

In this work, the partition coefficient of the plasticisers in two-phase systems has been calculated using the approach adopted by Sperling at al [47]. In the mathematical notation that will be used in the following equations, the *A* subscript will be referred to PLA, the *B* subscript will be referred to PBAT and the subscript *P* will be referred to the ATBC plasticiser.

For the PLA plasticised system Eq. (2) can be adopted [47,53,54] as follows:

$$T_{gA} = T_{gA,0} + w_{pA}p_A \tag{3}$$

where, the T_{gA} is the glass transition temperature of PLA in presence of plasticiser (ATBC), $T_{gA,0}$ is the T_g of pure unplasticised PLA, w_{pA} is the weight percent of ATBC plasticiser in PLA (polymer A); p_A corresponds to the plasticisation coefficient of the plasticiser P in the polymer A (that also corresponds to the slope of T_{gA} vs. w_{pA} plot) and is equal to:

$$p_A = \frac{T_{gP} - T_{gA,0}}{100} \tag{4}$$

Similarly, for the PBAT plasticised system:

$$T_{gB} = T_{gB,0} + w_{pB}p_B \tag{5}$$

$$p_B = \frac{T_{gP} - T_{gB,0}}{100} \tag{6}$$

where, T_{gB} is the glass transition temperature of PBAT in the presence of plasticiser (ATBC), $T_{gB,0}$ is the T_g of pure unplasticised PBAT, w_{pB} is the weight percent of ATBC plasticiser in PBAT (polymer B) and p_B corresponds to the plasticisation coefficient of the plasticiser P in the polymer B. Therefore, for plasticised PLA/PBAT or PBAT/PLA binary systems, it is possible to define a partition coefficient, $K_{A/B}$, (Eq. (7)) which indicates how the ATBC plasticiser will partition in between the two polymers A and B (PLA and PBAT):

$$K_{A/B} = \frac{w_{pA}}{w_{pB}} \tag{7}$$

Furthermore, it is possible to denote the overall weight percent of plasticiser P in the polymeric binary system as follows:

$$W_p = w_{pA}a + w_{pB}b \tag{8}$$

where, a and b are the weight fraction of polymers A and B in the binary blends, respectively. It should be noted that for an unplasticised binary system, $a+b = 1$.

In order to obtain a quantitative evaluation of $K_{A/B}$, the drop of the T_g and its dependence from the plasticiser composition can be written as follows for the polymeric binary blend system:

$$T_{gA} = T_{gA,0} + W_{pA}p_{A,a} \tag{9}$$

where, $p_{A,a}$ is the plasticisation coefficient of ATBC for the polymer *A* (PLA) in the system containing both A and B polymers; $p_{A,a}$ can be calculated as the slope of T_{gA} vs. W_p plot. By comparing Eqs. (3) and **(9)**:

$$w_{pA}p_A = W_{pA}p_{A,a} \tag{10}$$

Thus, for polymers A and B, it is possible to write that:

$$w_{pA} = W_p\left(\frac{p_{A,a}}{p_A}\right) \tag{11}$$

$$w_{pB} = W_p\left(\frac{p_{B,b}}{p_B}\right) \tag{12}$$

$$R_a = \sqrt{4\left(\delta_{D,ATBC} - \delta_{D,PLAorPBAT}\right)^2 + \left(\delta_{P,ATBC} - \delta_{P,PLAorPBAT}\right)^2 + \left(\delta_{H,ATBC} - \delta_{H,PLAorPBAT}\right)^2} \tag{17}$$

By applying Eqs. (11) and **(12)** to Eq. **(7)**:

$$K_{A/B} = \frac{p_{A,a}}{p_A} \Big/ \frac{p_{B,b}}{p_B} = \frac{p_{A,a}\cdot p_B}{p_{B,b}\cdot p_A} \tag{13}$$

Since the parameters that appear on the right-hand side of Eq. (13) can be obtained experimentally, the partition coefficient ($K_{A/B}$) can also be calculated.

2.3. Hansen solubility parameter (HSP) methodology

Hansen solubility parameters (HSPs) are the numerical values connected to the energies or intermolecular cohesive forces of binding molecules in a substance. HSPs have been adopted not only for the determination of the solubility of a substance into another [49,58], but also for (i) the wettability characterisation of various surfaces [59,60], (ii) the determination of adsorption properties [61], (iii) the prediction of the polymers compatibility [62] and (iv) the optimisation of the filler dispersion in a polymeric matrix [48].

The square of the total (or Hildebrand) solubility parameter as the sum of the squares of Hansen components [63]:

$$\delta^2 = \delta_D^2 + \delta_P^2 + \delta_H^2 \tag{14}$$

Consequently, any molecular substance can be identified by a point in a three-dimensional space (called Hansen space) in which the x, y and z axis correspond to δ_D, δ_P and δ_H respectively. Inside the Hansen space, both the solute and solvent can be identified by their HSPs (δ_D, δ_P and δ_H). Moreover, a solute can also be represented by an interaction radius (R_0) that corresponds to the radius of a sphere, having the centre coordinates equal to the HSPs [49]. The substances having a good affinity and qualified as "good solvents" for the solute stay within the solute sphere, while the substances having a low affinity and qualified as "nonsolvents" stay outside of the solute sphere.

For this purpose, the general parameter that conventionally adopted to compare two substances (denoted as 1 and 2) is the solubility parameter distance (R_a), which can be easily calculated (according to Eq. (15)) if the HSPs of the two components are known:

$$R_a = \sqrt{4(\delta_{D2} - \delta_{D1})^2 + (\delta_{P2} - \delta_{P1})^2 + (\delta_{H2} - \delta_{H1})^2} \tag{15}$$

In Eq. (15), the number 4 was introduced as a convenient factor in order to visualise the spherical regions of solubility rather than ellipsoidal [64]. The Relative Energy Difference (RED) can be used to quantify the distance between R_a and the interaction radius R_0 (Eq. (16)):

$$RED = \frac{R_a}{R_0} \tag{16}$$

It can be observed that for a good solubility or high affinity, must be $R_a < R_0$: consequently, the $RED < 1$ indicates the high solute-solvent affinity, while the RED >1 or a RED around 1 is equivalent to no energy difference or in a boundary condition.

In this work, the *HSPs* and R_0 values for both the polymers investigated (PLA and PBAT) and the HSPs values for the plasticiser used (ATBC) have been taken from literature [65,66] and reported in Table 6.

The solubility/affinity of ATBC in PLA and PBAT has been calculated by rewriting Eq. (17) as follows [65]:

Closer the RED value towards zero, better will be the affinity/compatibility; and if the RED value is higher than 1, then it indicates a theoretical immiscibility (null affinity) of the plasticiser with the matrix.

Table 1
Blends name and composition.

Pure plasticised blends composition			
Pure plasticised PLA blend name	PLA-ATBC wt.%	Pure plasticised PBAT blend name	PBAT-ATBC wt.%
PLA	100–0	PBAT	100–0
PLA5	95–5	PBAT5	95–5
PLA10	90–10	PBAT10	90–10
PLA15	85–15	PBAT15	85–15
PLA20	80–20	PBAT20	80–20
Binary plasticised blends composition			
Plasticised PLA/PBAT blend name	**(PLA80_PBAT20) wt.% - ATBC wt.%**	**Plasticised PBAT/PLA blend name**	**(PBAT80_PLA20) wt.% - ATBC wt.%**
PLA/PBAT	100–0	PBAT/PLA	100–0
PLA/PBAT_5	95–5	PBAT/PLA_5	95–5
PLA/PBAT_10	90–10	PBAT/PLA_10	90–10
PLA/PBAT_15	85–15	PBAT/PLA_15	85–15
PLA/PBAT_20	80–20	PBAT/PLA_20	80–20

Table 2
Process parameter values of blends extrusion.

Blends		Extruder Temperature profile (°C)	Ph (bar)
Pure plasticised PLA	PLA PLA5 PLA10 PLA15 PLA20	150/175/180/180/180/185/185/185/185/185	from 10 to 5
Pure plasticised PBAT	PBAT PBAT5 PBAT10 PBAT15 PBAT20	150/155/155/160/160/155/150/150/150/145/145 150/155/155/155/150/150/145/145/140/140/140	from 10 to 5
Plasticised PLA/PBAT	PLA/PBAT PLA/PBAT_5 PLA/PBAT_10 PLA/PBAT_15 PLA/PBAT_20	150/165/170/170/170/165/160/160/155/155/155 150/165/160/160/160/155/155/155/150/145/140	from 10 to 5
Plasticised PBAT/PLA	PBAT/PLA PBAT/PLA_5 PBAT/PLA_10 PBAT/PLA_15 PBAT/PLA_20	150/155/165/165/165/160/160/160/150/150/150 150/150/160/160/160/155/155/155/145/145/145	from 10 to 5

3. Experimental

3.1. Materials

Poly(lactic) acid (PLA) 3100HP was purchased from Natureworks LLC (Minnesota, USA), a medium viscosity PLA designed for medium flow injection moulding applications. It is a biodegradable polymer derived from natural sources that appears as white spherical pellets [density: 1.24 g/cm^3; melt flow index (MFI) (210 °C/2.16 kg): 24 g/10 min, Mw = 148,250 g/mol]. Poly(butylene adipate-co-terephthalate) (PBAT) Ecoflex®C1200 purchased from BASF (Ludwigshafen, Germany) is a biodegradable, aliphatic-aromatic copolyester based on the monomers 1.4-butanediol, adipic acid and terephthalic acid. Ecoflex®C1200 was supplied in the form of white spherical pellets [density: 1.26 g/cm^3, MFI (190 °C/2.16 kg): 3.8 g/10min, Mw = 105,000 g/mol].

Table 3
Injection moulding conditions.

Main injection moulding parameters	Pure plasticised PLA blends	Pure plasticised PBAT blends	Plasticised PLA/PBAT blends	Plasticised PBAT/PLA blends
Temperature profile (°C)	185/190/190	185/190/190	185/190/190	185/190/190
Mould temperature (°C)	from 60 to 50	55	from 60 to 50	55
Injection holding time (s)	10	10	10	10
Injection pressure (bar)	from 100 to 90	from 90 to 80	from 90 to 80	from 90 to 80
Cooling time (s)	25	25	25	25

Acetyltributylcitrate (ATBC) purchased from Tecnosintesi (Bergamo, Italy) is a safe, non-toxic, biodegradable and biobased plasticiser, which appears colourless and odourless oily liquid [density: 1.05 g/cm^3, Mw: 402.5 g/mol].

3.2. Blends and samples preparation

PLA and PBAT pellets were dried in a Piovan DP 604-615 dryer (Piovan S.p.A., Verona, Italy) at 60 °C for 8 h before processing. Blends were extruded according to the compositions reported in Table 1, in which the plasticised PLA/PBAT blends were composed by a PLA matrix (80 wt%) with PBAT as dispersed phase (20 wt%), while the plasticised PBAT/PLA blends were composed by a PBAT matrix (80 wt%) with PLA as dispersed phase (20 wt%). The ratio between the two polymers was maintained the same and different quantities of plasticiser were added (from 5 to 20 wt%).

All the blends were processed with a semi-industrial Comac EBC 25HT (L/D = 44) (ComacS.r.l., Cerro Maggiore, Italy) twin-screw extruder, equipped with a principal feeder for pellets and a peristaltic pump to feed the plasticiser. For all the blends, the screw speed was set at 250 rpm and the total mass flow rate was kept at 18 kg/h. The temperature profiles of the 11 zones of the extruder are reported in Table 2. It can be observed that, due to the viscosity decrement caused by the plasticiser amount, the temperature profile set has been decreased for all the blends when the amount of plasticiser reaches at least 15 wt%.

The strands coming out from the extruder dies were cooled in a water bath at room temperature and shaped into pellets by an automatic knife cutter. The pellets were then finally dried at 30 °C for 8 h using the PIOVAN dryer.

In order to perform the tensile tests for determining the mechanical properties, all the blends were processed with an injection moulding press Megatech H10/18–1 (TECNICA DUEBI S.r.l, Fabriano, Italy). Dog bone specimens according to ISO 527-1A (with a dimension of 80 x 10 × 4 mm) were obtained. The injection moulding parameters adopted are reported in Table 3. In order to obtain the injection moulded specimens having the conditions as close as possible to each other, the same injection temperature profile for all the blends was adopted. Since PLA is the polymer that melts at higher temperatures, the injection moulding profile of PLA was chosen, since at these temperatures, the PBAT also exhibits a good melt strength making it suitable to injection moulding process. The mould temperature was also comparable for all the blends. However, it was observed that, for the pure plasticised PBAT blends and the plasticised PBAT/PLA blends, it was possible to set the same mould temperature (equal to 55 °C). On the other hand, for the pure plasticised PLA blends and plasticised PLA/PBAT blends, the mould temperature was decreased with the ATBC amount from 60 to 50 °C. The injection pressure was also gradually decreased with the increasing of ATBC content due to the lowering of melt viscosity [45,67,68].

3.3. Mechanical characterisations

Tensile tests were performed after 3 days of the injection moulding process; the specimens were stored in a dry keeper (SANPLATEC Corp., Osaka, Japan) at controlled atmosphere (room temperature and 50% r. h). At least ten specimens were tested and the average values of the main mechanical properties (Young's modulus, yield stress, stress at break and elongation at break) were reported. Static tensile tests were conducted at room temperature at a cross speed of 10 mm/min with an MTS Criterion 43 universal testing machine (MTS Systems Corporation, Eden Prairie, MN, USA), equipped with a 10 kN load cell and interfaced with an MTS Elite Software (MTS Testsuite version 4.1).

3.4. Thermomechanical characterisations

Dynamic mechanical thermal analysis (DMTA) was carried out to evaluate the glass transition temperatures of all the blends, with a GABO Eplexor® 8 (Gabo Qualimeter GmbH, Ahlden, Germany) equipped with a load cell of 100 N and liquid nitrogen was used to cool the chamber with the tensile configuration. Tests were carried out on injection moulded specimens with a dimension of 50 x 10 × 4 mm, obtained from the useful section of the dog bone specimens (ISO 527-1A). The speed rate of 2 °C/min and the frequency of 1 Hz were set, in different temperature ranges varying from 0 to 100 °C for pure plasticised PLA blends, from −80 to 60 °C for pure plasticised PBAT blends and from −80 to 100 °C for the two binary blend systems with plasticiser. DMTA experiments were carried out in duplicate and the relaxation temperature, associated with the glass transition, was taken at the maximum of the peak of the damping factor ($tan\delta$).

In order to apply the analytical models explained in section 2.1 and 2.2, the DMTA technique was used to measure the glass transition variation since the response of the viscoelastic modulus is generally more sensitive than the small variation in heat capacity measured by the differential scanning calorimetry (DSC). In fact, the decrease in the storage modulus (E') signal during the glass transition phase is often of several orders of magnitude (even if small quantities of amorphous phase are present) and thus can be easily detected [69].

3.5. Thermal characterisation

Differential scanning calorimetry (DSC) measurements were carried out with a TA Q200 (TA Instruments, New Castle, UK) equipped with RSC90 cooling system, in order to evaluate the crystallinity of blends after the injection moulding process. Indium was used as the standard for the calibration with aluminium hermetic pans. Nitrogen was used as purge gas set at a rate of 50 mL/min. The samples were obtained by cutting them into small pieces (about 10–15 g) of materials and sealing them inside the aluminium pans. The sampling was carried out exactly in the same region of the injection moulded specimens to avoid differences ascribable to different cooling rates in the specimen thickness. In order to take into account the final properties of materials after the injection moulding process, the thermal history of the materials has been considered and consequently the thermal properties and the crystallinity were evaluated considering only the first DSC heating scan. All the blends were subjected to the same method: a quick cooling from room temperature to −60 °C (this temperature was maintained for 1 min) followed by a heating ramp up to 200 °C with a rate of 10 °C/min.

Glass transition temperature (T_g), melting temperature (T_m), cold crystallisation temperature (T_{cc}) and the enthalpies of melting and cold crystallisation for PLA and/or PBAT were determined directly from the DSC thermograms. The melting temperature and the cold crystallisation temperature of the polymers were recorded at the maximum of the melting peak and at the minimum of the cold crystallisation peak, respectively. The enthalpies of melting (ΔH_m) and cold crystallisation (ΔH_{cc}) were determined from the corresponding thermograms peak areas.

Table 4
Tensile mechanical properties for pure plasticised materials and plasticised PLA/PBAT and PBAT/PLA binary blends.

Blend Name	Young's Modulus (MPa)	Yield stress (MPa)	Stress at break (MPa)	Elongation at break (%)
PLA	3,200 ± 100	-	69.0 ± 0.3	2.2 ± 0.1
PLA5	2,900 ± 100	-	55.7 ± 0.3	3.6 ± 0.1
PLA10	2,800 ± 100	-	49.1 ± 1.2	3.5 ± 0.2
PLA15	2,600 ± 100	40.9 ± 1.0	19.2 ± 2.4	235.7 ± 28.9
PLA20	700 ± 100	5.0 ± 1.1	24.2 ± 1.2	473.2 ± 18.8
PLA/PBAT	2,500 ± 100	51.4 ± 1.0	27.9 ± 2.3	254.8 ± 25.0
PLA/PBAT_5	2,300 ± 100	40.8 ± 0.7	30.7 ± 3.1	365.6 ± 28.8
PLA/PBAT_10	2000 ± 100	31.3 ± 0.6	21.5 ± 2.9	378.0 ± 22.4
PLA/PBAT_15	1,200 ± 100	5.8 ± 0.6	20.0 ± 0.7	443.4 ± 39.5
PLA/PBAT_20	400 ± 100	2.8 ± 0.4	17.2 ± 1.3	503.1 ± 19.2
PBAT	100 ± 10	7.1 ± 0.1	No break	No break
PBAT5	70 ± 10	6.4 ± 0.1		>500%
PBAT10	50 ± 10	5.6 ± 0.1		
PBAT15	40 ± 10	5.0 ± 0.1		
PBAT20	30 ± 10	4.0 ± 0.1		
PBAT/PLA	310 ± 10	9.9 ± 0.3	No break	No break
PBAT/PLA_5	280 ± 10	7.3 ± 0.1		>500%
PBAT/PLA_10	190 ± 10	5.4 ± 0.1		
PBAT/PLA_15	120 ± 10	5.2 ± 0.1		
PBAT/PLA_20	80 ± 10	5.0 ± 0.1		

The percentage of crystallinity of PLA and PBAT in the blends (X_{cc}) was calculated according to the equation (**Eq. (20)**) [45,70]:

$$X_{CC\ (PLAorPBAT)} = \frac{\Delta H_{m(PLA\ or\ PBAT)} - \Delta H_{CC(PLA\ or\ PBAT)}}{\Delta H^{0}_{m\ (PLA\ or\ PBAT)} \cdot wt.\%_{PLA\ or\ PBAT}} \cdot 100 \quad (18)$$

where, the ΔH°_m is the theoretical melting heat of 100% crystalline polymer. For PLA a ΔH°_m value of 93 J/g [71] and for PBAT a ΔH°_m value of 114 J/g were considered [72].

For the binary blends, it must be pointed out that the value of ΔH_{cc} of PLA (for the PLA/PBAT blends) and the value of ΔH_m of PBAT (for the PBAT/PLA blends) are affected by the partial overlap between the latent heat of PBAT melting and the PLA cold crystallisation; consequently, the values of X_{cc} for the plasticised PLA/PBAT and PBAT/PLA blends are slightly underestimated. However, these values are useful to evaluate the effect of both the plasticiser and the dispersed phase in the binary injection moulded blends [73].

3.6. Optical analysis

Morphological analysis of the plasticised binary system blends was carried out with FEI Quanta 450 FEG scanning electron microscope (SEM) (Thermo Fisher Scientific, Waltham, MA USA). The SEM analysis was performed on cryo-fractured samples of the dog bone specimens. The samples surfaces were sputtered with platinum, with a LEICA EM ACE 600 High Vacuum Sputter Coater (Leica, Wetzlar, Germany), in order to avoid charge build-up. The analysis was carried out under high-vacuum system conditions and the images were chosen (at 10.000 X) to evaluate the effect of plasticiser and dispersed phase of the binary blends.

4. Results and discussion

4.1. Mechanical characterisations

The main mechanical properties of the plasticised systems

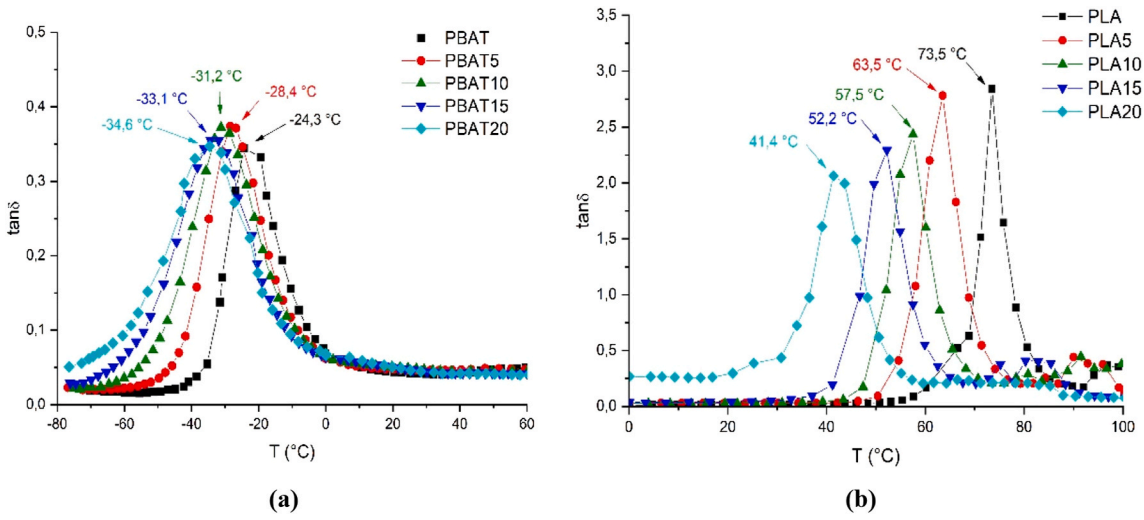

Fig. 1. Variation of damping factor (tan δ) with temperature for: (**a**) pure plasticised PLA and (**b**) pure plasticised PBAT blends with T_g values indicated.

Table 5
T_g values of PLA and PBAT obtained from the DMTA analysis.

Blend name	T_g (°C) from DMTA	T_g (°C) according to Fox equation
PLA	73.5	-
PLA5	63.5	59.9
PLA10	57.5	47.3
PLA15	52.2	35.6
PLA20	41.4	24.8
PBAT	−24.3	-
PBAT5	−28.4	−28.0
PBAT10	−31.2	−31.7
PBAT15	−33.1	−35.2
PBAT20	−34.6	−38.8

investigated in this work are summarised in Table 4.

From the mechanical point of view, PLA and PBAT have a different behaviour. PLA is a rigid material that exhibits brittle failure (no yield and low elongation at break), while PBAT has a rubber-like behaviour and for this reason it was observed no occurrence of breakage and the tensile test machine reached the end of its stroke. However, as it can be expected, with the increase of ATBC content, the decrement of both the yield stress and the Young's modulus and a ductility increment were observed. Further, it was interesting to observe the change in the PLA20 mechanical response, where the tensile strength was similar to that of the PBAT and its blends. In any case for both the polymers, the mechanical behaviour is coherent to what was expected and also reported in literature [69,70] with a reduction of brittleness and enhancement of elongation with the increasing amount of ATBC.

The decrease of the Young's modulus and the contemporary increment of elongation at break with the ATBC content were also observed for the plasticised PLA/PBAT and PBAT/PLA binary blends. The tensile behaviour of PLA/PBAT blends shows how the PLA mechanical response changes with the introduction of the PBAT dispersed phase. A remarkable growth in elongation at break (from 2.2 to 254.8%) was observed and it was in-line with the literature values [12,22,74,75], in which the dispersed PBAT particles act as tougheners according to the rubber toughening theory [76,77]. On the other hand, the presence of PLA dispersed particles inside the PBAT matrix of the PBAT/PLA binary blend does not alter the mechanical response of the blend in a significant way rather it is only a slight stiffer (the Young's modulus passes from 0.1 GPa for pure PBAT to 0.31 GPa for PBAT/PLA blend), but it still behaves similar to PBAT with a rubber-like response.

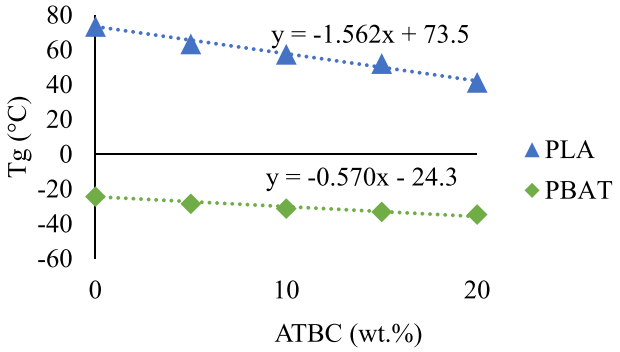

Fig. 2. T_g values of PLA and PBAT in pure plasticised materials from DMTA analysis with their linear regression.

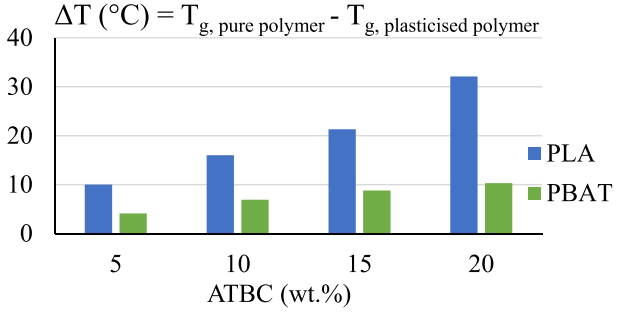

Fig. 3. Difference between the glass transition temperature of pure PLA and PBAT with the corresponding plasticised polymers with increasing ATBC content.

4.2. Results for pure plasticised PLA and PBAT materials

The variation of the damping factor with temperature for both pure plasticised PLA and PBAT blends is reported in Fig. 1. The relaxation temperatures correlated to the glass transition temperatures (taken at the maximum of the *tan δ* peak [69,78]) are reported in Table 5.

For both the polymer systems, a shift towards lower temperature and a broadening of the width of the *tanδ* peak with the increasing ATBC content are detected. For PLA blends, a slight increment of damping factor in proximity of the PLA cold crystallisation temperature (80 °C) is also observed [69].

Table 6
PLA, PBAT and ATBC HSPs, PLA and PBAT interaction radius (R_0), PLA and PBAT calculated solubility parameter distance (R_a) and PLA and PBAT Relative Energy Difference (RED).

	δ_d ($J^{1/2} \cdot cm^{-3/2}$)	δ_p ($J^{1/2} \cdot cm^{-3/2}$)	δ_H ($J^{1/2} \cdot cm^{-3/2}$)	R_0	R_a	RED
PLA	18.60	9.90	6.00	10.70	8.12	**0.76**
PBAT	18.55	4.90	7.82	3.90	3.97	**1.02**
ATBC	16.90	2.70	7.60	-	-	-

The low molecular size of the plasticiser allows it to occupy the intermolecular spaces between the polymer chains, reducing the energy for the molecular motion and the formation of hydrogen bonding between the polymer chains, which in turn increases the free volume and molecular mobility to reduce the glass transition temperature [78]. The shift temperature of the *tan δ* is more pronounced for PLA as compared to that of the PBAT as it can be observed from Table 5. As expected, the glass transition temperature decreases with the amount of plasticiser in both PLA and PBAT matrices, agreeing with literature [78]. It can be observed that by increasing the ATBC content, the plasticiser is more effective in reducing the T_g of PLA than that of the PBAT.

In Table 5, the results obtained by the application of the Fox equation (Eq. (1)) are also reported; the T_g data for PLA and PBAT have been taken from the DMTA results, while the ATBC T_g value has been taken from the literature, which is to be −82.4 °C [22].

The Fox equation does not predict well the T_g trend with the plasticiser content. The discrepancy between the predicted T_g value and the experimental data is even more pronounced as the ATBC content increases. In fact, for both the polymers, the greatest variation of T_g is observed for small additions of ATBC. However, this trend is not dissimilar from what is reported in the literature [69,79].

On the other hand, both PLA and PBAT systems show a linear dependence of glass transition temperature by the ATBC content and thus Eq. (3) and Eq. (5) can be adopted for PLA and PBAT, respectively. Performing the linear regression of the T_g vs ATBC content plot (as shown in Fig. 2), the values of the slopes of the straight lines (corresponding to p_A and p_B) can be calculated.

For PLA, the p_A value of −1.562 was obtained, while for the PBAT,

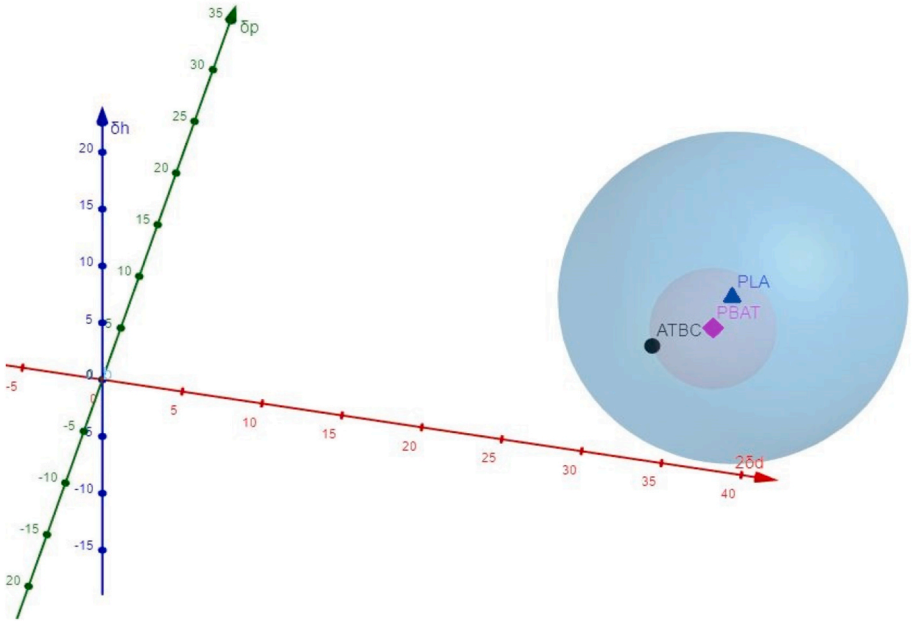

Fig. 4. Representation of ATBC (black circular point) polymer solubility sphere in Hansen space. The PLA solubility sphere (outer light blue sphere) is centred in the blue triangular point, while the PBAT solubility sphere (inner light fuchsia sphere) is centred in the fuchsia rhomboidal point. (For interpretation of the references to colour in this figure legend, the reader is referred to the Web version of this article.)

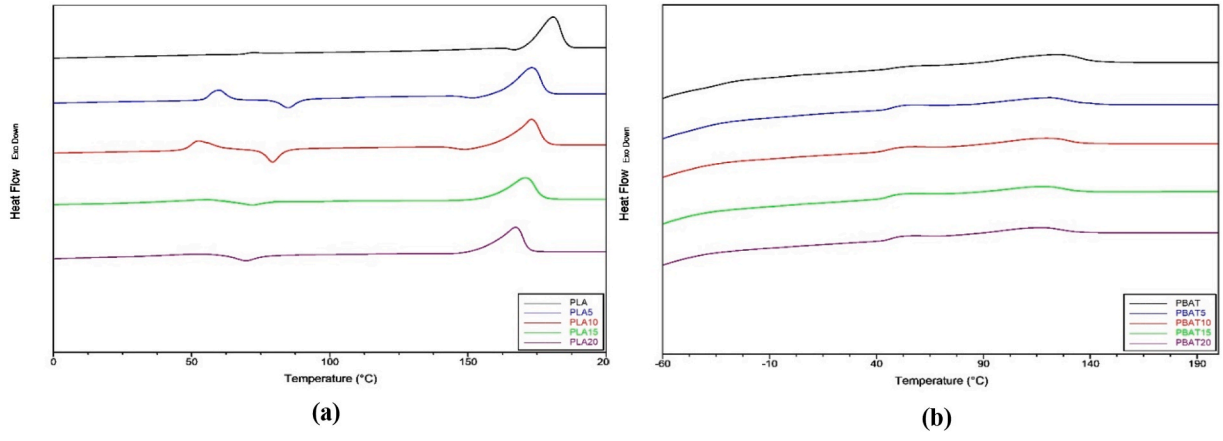

Fig. 5. DSC first heating thermograms for (**a**) PLA based system and (**b**) PBAT based system.

Table 7
DSC first heating results for pure plasticised PLA and PBAT blends.

Blend name	T_g (°C)	Tm (°C)	T_{cc}(°C)	ΔH_m (J/g)	ΔH_{cc} (J/g)	X_{cc} (%)
PLA	57.1	180.8	-	45.7	-	49.2
PLA5	45.8	173.2	84.9	46.5	8.0	43.5
PLA10	36.4	172.9	79.4	44.1	9.4	41.4
PLA15	26.2	170.9	72.3	43.1	8.1	44.2
PLA20	19.5	167.4	71.8	43.0	9.0	45.8
PBAT	−30.6	122.6	-	23.2	-	33.1
PBAT5	−36.6	120.7	-	16.4	-	27.4
PBAT10	−42.6	115.7	-	15.1	-	27.2
PBAT15	−45.6	116.6	-	12.4	-	30.4
PBAT20	−46.1	111.5	-	12.0	-	32.2

the p_B was found to be −0.57. The more marked displacement in T_g with the ATBC content for the PLA system rather than PBAT system (Fig. 3) is reflected in a higher value of p_A with respect to p_B. This result leads to hypothesise a greater affinity of ATBC towards PLA rather than PBAT or to a probably lower solubility limit of ATBC in PBAT rather than in PLA. The greater variation in T_g for the PLA-based system is also reflected in the injection moulding conditions (Table 3): in fact, with the ATBC increment, the mould temperature was never changed for the PBAT blends, while, it was lowered for the PLA blends.

The calculation of the solubility parameter distance (R_a) (according to Eq. (17)) as well as the Relative Energy Difference (*RED*) (according to Eq. (18)) were calculated from the HSPs; the polymer interaction radius (R_0) values were taken from literature [65,66] and reported in Table 6.

A better affinity between PLA and ATBC can be encountered; in fact, for the PLA-ATBC system, the RED is equal to 0.76 (RED <1) indicating a high solute-solvent affinity if compared to PBAT-ATBC system for which the RED equal to 1.02 was obtained. In particular, being the RED value for PBAT-ATBC system slightly higher than 1, a theoretical partial immiscibility (or very low affinity) of the ATBC with the PBAT is expected. Accordingly, the data obtained are in agreement with the T_g trend and confirmed a better affinity of ATBC towards PLA than PBAT. In particular, thanks to the representation of the ATBC and the polymers in the Hansen space (Fig. 4), it can be observed that the ATBC totally lies within the PLA solubility sphere and consequently, the ATBC is fully soluble/affine to PLA. Nevertheless, the PBAT sphere of solubility is smaller as compared to that of PLA and the ATBC lies exactly in the border of the PBAT sphere solubility, leading to a poor solubility/affinity between ATBC and PBAT. These obtained results are in accordance with the observations reported by Labrecque et al. [19], who studied the effect of citrate plasticisers into a PLA matrix and they found that the citrate plasticisers were miscible with PLA due to the polar interactions between the ester groups of PLA and the plasticiser.

For the further confirmation of the data obtained, it was observed that the PBAT specimens, having an ATBC content greater than 10 wt%, began to exude plasticiser after some weeks after the injection moulding, while the PLA specimens did not exude plasticiser in any case.

In order to exclude the possible influence of a different crystallinity content between the two polymers, which could possibly contribute to plasticiser specimen migration [14], the first heating DSC thermograms obtained directly on the injection moulded specimens were analysed and

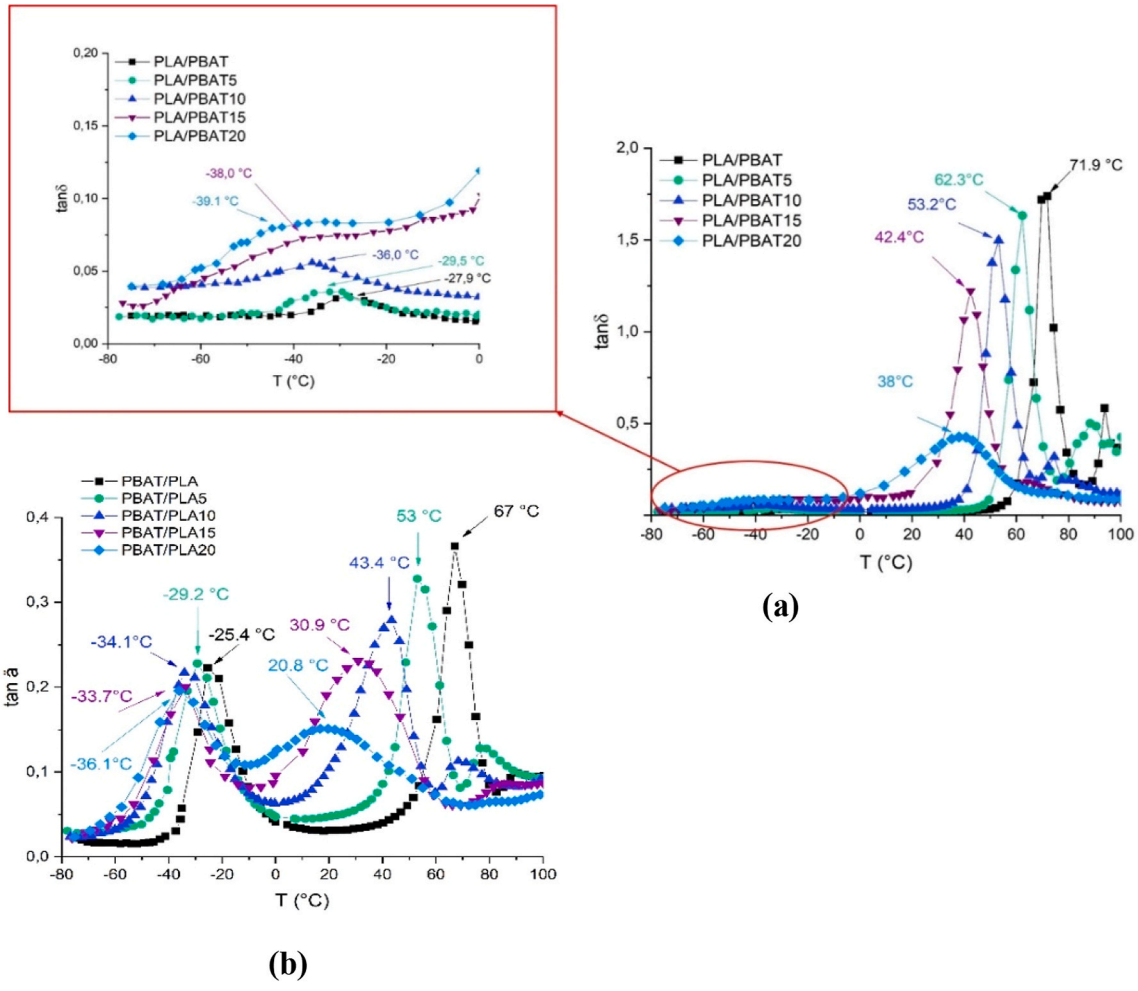

Fig. 6. Variation of damping factor (*tan δ*) with temperature for: (**a**) PLA/PBAT blends and(**b**) PBAT/PLA blends.

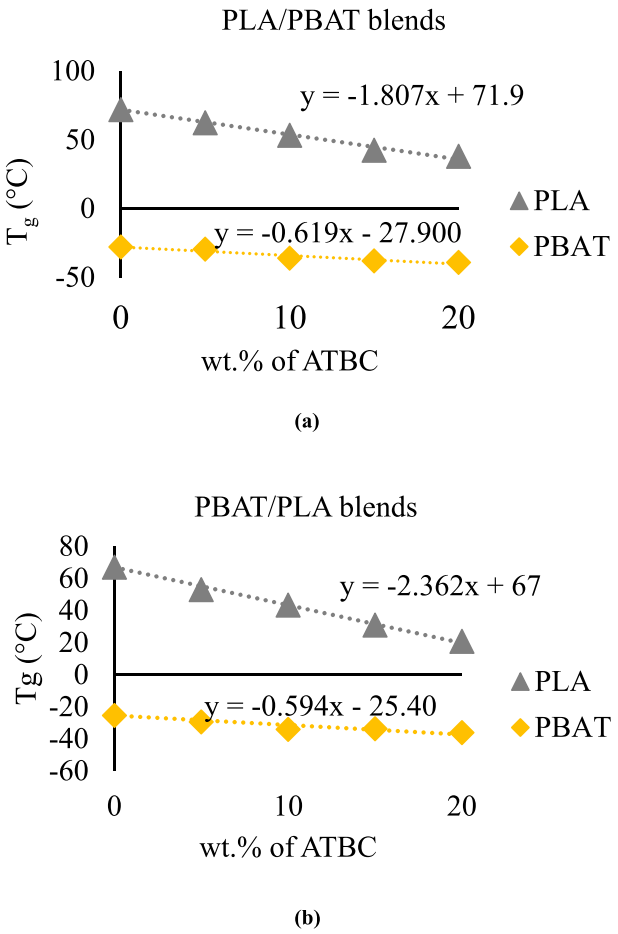

Fig. 7. Linear regression of T_g values of PLA and PBAT vs. ATBC content in PLA/PBAT (a) and PBAT/PLA (b) plasticised blends from DMTA analysis.

the results are reported in Fig. 5 and Table 7.

DSC confirmed the decrement in the glass transition temperature of PLA with the ATBC content, however an enthalpic relaxation peak above the PLA glass transition temperature due to the PLA aging was observed [80]. The addition of ATBC affects both the PLA cold crystallisation temperature (T_{cc}) and melting temperature (T_m), causing a shift towards lower temperature as confirmed by the results observed in other similar cases [20,78].

As far as concern PBAT blends, also in this case a decrement of the glass transition temperature with the ATBC content was observed; however, starting from PBAT10, the low variation in the DSC signal did not allow a great accuracy in the T_g determination. The melting

Table 8
Plasticiser coefficients ($p_{A,a}$ and $p_{B,b}$), partition coefficient ($K_{A/B}$) and weight percentage (w_{pPLA} and w_{pPBAT}) of ATBC in PLA and PBAT in the binary blends (PLA/PBAT and PBAT/PLA).

				ATBC content in plasticised binary blends (wt.%)			
				5	10	15	20
PLA/PBAT blends	$p_{A,a}$ = −1.807 $p_{B,b}$ = -0.619	$K_{A/B}$ = 1.07	w_{pPBAT}	0.048	0.095	0.143	0.190
			w_{pPLA}	0.051	0.101	0.152	0.202
PBAT/PLA blends	$p_{A,a}$ = −2.362 $p_{B,b}$ = -0.594	$K_{A/B}$ = 1.45	w_{pPBAT}	0.046	0.092	0.138	0.183
			w_{pPLA}	0.067	0.133	0.200	0.266

behaviour of PBAT is consistent with the literature [72], showing two endothermic peaks centred at around 55 and 122.59 °C; the first peak is generally attributed to the melting of the crystalline phase of BA fraction present in the sample [81]. The thermal behaviour of the PBAT with the addition of ATBC is similar to what is being observed for PLA, where the melting temperature decreases with the ATBC amount.

For both PLA and PBAT, the larger chain mobility induced by the ATBC causes an increment of the crystallinity with the ATBC content. However, it is interesting to note (from Table 7) that the highest crystallinity was observed for the PLA-based compounds, which have an average crystallinity degree of about 45%. The PBAT blends have a slightly lower average crystallinity degree of about 30%. The data obtained therefore lead to exclude the influence of crystallinity on the plasticiser migration observed for some PBAT blends composition (from 10 wt% of ATBC on). In fact, since the plasticiser goes into the amorphous phase, being the amorphous region smaller for PLA than PBAT and assuming the same affinity between ATBC and two polymers, there could be a migration of the plasticiser from the PLA-based compounds rather than from the PBAT-based compounds [14]. This migration is therefore linked to the major/minor affinity between the polymer and the plasticiser.

By comparing PLA and PBAT based blends with the same ATBC content, the PBAT-based specimens are less crystalline than that of their PLA-based counterparts. Consequently, if the ATBC affinity is same for both the polymers, the effect of T_g variation with the plasticiser content would be same or greater for PBAT (having less crystalline fraction) than for PLA. Nevertheless, for the PLA systems, a more pronounced shift in the glass transition temperature with increasing amount of ATBC was encountered. This matched with the results obtained from the HSPs methodology, in which a greater affinity of ATBC in PLA was observed as compared to that of the PBAT.

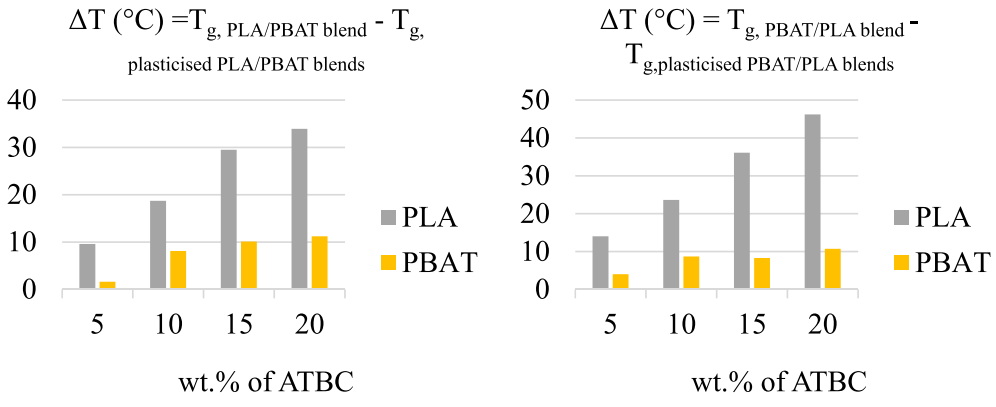

Fig. 8. PLA and PBAT Tg shift with the increasing of ATBC content in PLA/PBAT (left side) and PBAT/PLA (right side) systems from DMTA analysis.

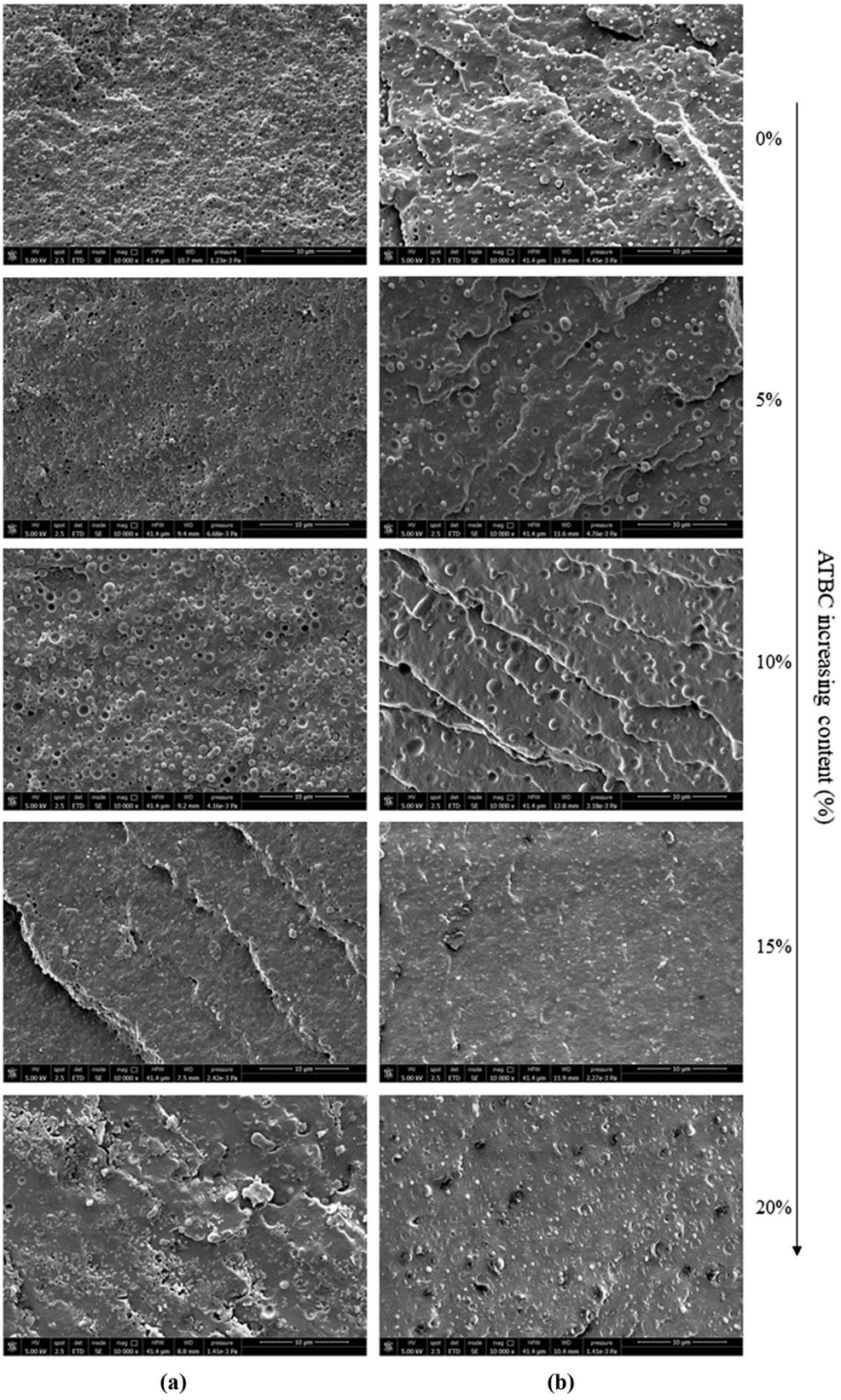

Fig. 9. SEM micrographs of **(a)** PLA/PBAT and **(b)** PBAT/PLA blends in comparison with ATBC increasing content.

4.3. Results for plasticised PLA/PBAT and PBAT/PLA blends

On the basis of the results obtained, it is expected a greater affinity of ATBC towards the PLA phase rather towards PBAT. In order to consider the effects of both morphology and of a smaller or larger quantity of one of the two polymers in the binary blends, it was decided to study two complementary systems: (i) a PLA-based system (PLA/PBAT with 80 wt % of PLA and 20 wt% of PBAT) and (ii) the corresponding PBAT-based

Table 9
DSC first heating results for plasticised PLA/PBAT and PBAT/PLA blends.

Blend name	T_g (°C)	T_m (°C)	T_{cc}(°C)	ΔH_m (J/g)	ΔH_{cc} (J/g)	X_{cc} (%)
PLA/PBAT	61.6	176.0	87.5	40.5	20.7	26.7
PLA/PBAT_5	57.4	174.3	78.8	36.8	14.3	31.9
PLA/PBAT_10	50.0	171.6	79.6	32.8	11.0	32.5
PLA/PBAT_15	47.9	169.2	79.6	29.3	6.4	36.3
PLA/PBAT_20	44.6	168.0	79.2	31.5	5.1	44.4
PBAT/PLA	-	118.4	-	7.8	-	12.6
PBAT/PLA_5	-	115.2	-	9.3	-	15.6
PBAT/PLA_10	-	113.0	-	7.3	-	13.6
PBAT/PLA_15	-	112.3	-	7.2	-	15.7
PBAT/PLA_20	-	112.1	-	6.8	-	12.9

system (PBAT/PLA with 80 wt% of PBAT and 20 wt% of PLA). For both the investigated systems, an increasing ATBC content from 5 to 20 wt% was also added.

From the observed DMTA *tanδ* peak variation (Fig. 6), it can be seen a greater shift in the T_g with ATBC content, which is therefore independent from the quantity of PLA present in the blend.

This emerged major shift in T_g for PLA can be better observed by performing the linear regression of the T_g vs ATBC content (Fig. 7), in which the values of the slopes of the straight lines (corresponding to $p_{A,a}$ and $p_{B,b}$ according to Eq. (9)) are higher for PLA rather than for PBAT for the both systems investigated.

For PLA, the value of $p_{A,a}$ was found to be −1.807 and −2.362 for PLA/PBAT and PBAT/PLA blends, respectively; while for the PBAT, the value of $p_{B,b}$ was found to be −0.619 and −0.594 for the PLA/PBAT and PBAT/PLA blends, respectively. The higher $p_{A,a}$ values are reflected in the more marked T_g shift with the ATBC content for PLA rather than PBAT, in both systems analysed (Fig. 8). The major PLA shift is clearly observed for PBAT/PLA blends, where the $p_{A,a}$ value is higher. Also in this case, the results obtained induce to a greater affinity of ATBC towards PLA rather than towards PBAT. To better clarify the results obtained for the binary compounds, it is therefore necessary to analyse the partition coefficient, $K_{A/B}$, that specifies how the ATBC plasticiser is portioned between the two polymers (PLA and PBAT). In Table 8, the main parameters, experimentally obtained and useful for the calculation of the partition coefficient, are calculated according to the procedure adopted by Sperling et al. [47] (Section 2.2).

A partition coefficient, $K_{A/B}$, equal to the value of 1 implies that the plasticiser is almost uniformly distributed between the two phases. It is interesting to note that for both systems analysed, the partition coefficient is higher than 1 ($K_{A/B}$ = 1.07 for PLA/PBAT system and $K_{A/B}$ = 1.45 for PBAT/PLA system), indicating a higher distribution of ATBC in the PLA phase rather than in PBAT. This result can also be observed by the values of the weight percentage of ATBC in PLA and PBAT in the binary blends (w_{pPLA} and w_{pPBAT} respectively). For all the ATBC contents, the w_{pPLA} is higher than the corresponding w_{pPBAT}, indicating a preferential distribution of the plasticiser towards PLA than PBAT and independent from the PLA/PBAT ratio in the blend.

However, for the PLA-based binary blends, the value of $K_{A/B}$ is slightly higher than 1 and in first hypothesis, this K value could be related to the greater quantity of PLA rather than PBAT. Nevertheless, by analysing the K value obtained for PBAT-based binary blends, it can be observed a clear preference of ATBC in the PLA phase. In fact, for these binary blends, the K value is higher, which is indicating that the concentration of ATBC is higher in the PLA phase than that of the PBAT phase, despite PLA is the minor phase. The analysis of the partition coefficient has therefore confirmed what has been observed so far, showing a greater affinity of ATBC in the PLA phase.

However, in order to better understand the $K_{A/B}$ values obtained, the morphology of the blends was also investigated. As it can be observed from the SEM images (Fig. 9), all the systems exhibit a typical two-phase structure, with dispersed droplets of the minor phase in the matrix. The ATBC addition results in an increase of the diameter of the dispersed phase. Notably, this phenomenon is in agreement with the literature [22,82] as well, in which the reduced viscosity induced by the addition of plasticiser leads to an increase of the dispersed domain diameter. In both the investigated binary blends, starting from 15 wt% of ATBC content, the dispersed particles become so close to each other, that they tend to coalesce forming larger domains (similar to small islands).

It can also be observed that the PLA particles dispersed in the PBAT matrix are larger than those of the PBAT dispersed in the PLA matrix. This phenomenon can be ascribable to several factors such as the difference in the viscosity ratio between the two polymers within the system, the shear stress generated during the extrusion and the interfacial tension between the two polymers. Furthermore, another important factor that determines the morphology of an immiscible blend is the viscoelasticity of the phases: the more the dispersed phase is highly elastic, the more difficult it is to break the micro droplets [83].

Similar to what was observed for the pure plasticised PBAT blends, the PBAT/PLA binary blends containing the amount of ATBC greater than 10 wt% showed the migration of ATBC after some weeks from the injection moulding process. In order to exclude the possible influence of different crystallinity contents between the two binary blends, which could possibly contribute to plasticiser migration, a DSC analysis of the

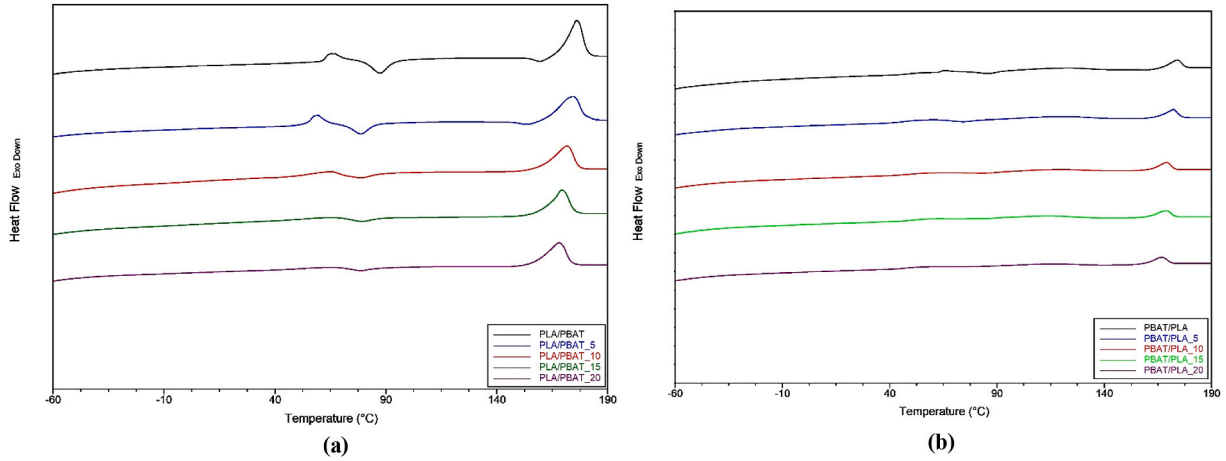

Fig. 10. DSC first heating thermograms for (**a**) PLA/PBAT-based system and (**b**) PBAT/PLA-based system.

injection moulded specimens was also carried out, considering the first heating scan.

The main DSC results, reported in Table 9, are referred to the main thermal characteristics of the matrix (PLA for PLA/PBAT system and PBAT for PBAT/PLA system).

For the PLA/PBAT blends, there is an overlap between the PBAT melting region and the PLA cold-crystallisation region [72](Fig. 10) that makes impossible the detection of the PBAT melting temperature; the ATBC addition caused a shift towards the lower temperatures of both cold crystallisation temperature (T_{cc}) and melting temperature (T_m). Interesting is to observe that the PBAT dispersed particles does not influence the PLA crystallinity that increases with the increasing ATBC amount from 26.72 to 44.41%.

As far as concern the PBAT/PLA blends, it was not possible to measure the variation of the PBAT glass transition temperature with the ATBC content with the required accuracy. Similarly, as what was observed for the corresponding pure plasticised PBAT blends, a decrease in the melting temperature is observed introducing the plasticiser. The crystallisation behaviour of the PBAT/PLA binary blends is similar to the pure plasticised PBAT blends, where the percentage of PBAT crystallinity is almost constant (around 14%).

The DSC results shows that the PLA/PBAT blends are more crystalline than that of the corresponding PBAT/PLA blends. Consequently, the PLA crystallinity seems to be not influenced by the plasticiser migration, that can be thus correlated to the poor affinity of ATBC towards the PBAT.

5. Conclusions

In this work the affinity of acetyl tributyl citrate plasticiser (ATBC) towards PLA and PBAT polymers was investigated.

Pure plasticised PLA and PBAT blends containing different amount of ATBC contents (from 5 to 20 wt%) were investigated. DMTA tests were carried out in order to evaluate the shift in the glass transition temperature (T_g) of the two polymers with the increasing amount of ATBC. The major shift in the T_g was observed for PLA rather than PBAT, which has led to the deduction of a greater affinity of the ATBC towards the PLA rather than the PBAT. The analysis of Hansen solubility parameters (HSPs), adopted for the determination of the ATBC solubility within the two polymers (PLA and PBAT) confirmed the experimental observations: ATBC lies entirely within the PLA solubility sphere, while it lies exactly in the border of the PBAT sphere solubility. Accordingly, it resulted in the poor solubility/affinity between ATBC and PBAT. DSC analysis was also performed to exclude the possible influence of the crystallinity of the two polymers.

The PLA/PBAT and PBAT/PLA binary blends containing different ATBC amounts (from 5 to 20 wt%) were also investigated. In particular, a PLA-based system (80 wt% PLA and 20 wt% PBAT) and a PBAT-based system (80 wt% of PBAT and 20 wt% of PLA) were carefully examined. The evaluation of the glass transition temperature through DMTA test revealed, also in this case, a longer affinity of ATBC towards PLA for both the binary systems investigated. The calculation of the plasticiser partition coefficient for both the system analysed revealed that the partition coefficient is higher than 1 ($K_{A/B} = 1.07$ for PLA-based system and $K_{A/B} = 1.45$ for PBAT-based system) indicating a larger distribution of ATBC in the PLA phase rather than PBAT. Moreover, the varying weight percentages of ATBC in PLA in the binary blends, which is higher than the corresponding ATBC weight percentage in PBAT, indicated a preferential distribution of the plasticiser towards PLA than PBAT (independent of the PLA/PBAT ratio in the blend). In addition, the DSC analysis was also performed for these binary systems to exclude the effects of crystallinity in influencing the ATBC distribution. In particular, it was observed that the crystallinity of PBAT-based system was lesser than that of its corresponding PLA-based system and thus ideally, if the affinity between the two polymers were the same, the plasticiser should go in greater quantity towards more amorphous polymer (PBAT). Nevertheless, since the affinity between the two polymers was not same, a major quantity of ATBC was encountered in PLA (even if more crystalline).

The morphology of the binary blends was also investigated. For both the binary blends, the dispersed particles of the minor phase were found to be embedded in the matrix (major phase). Further, with the increasing ATBC amount, an increase in the dispersed domains diameter was also observed due to the addition of the plasticiser.

Funding

No funding was received for this work.

Intellectual property

We confirm that we have given due consideration to the protection of intellectual property associated with this work and that there are no impediments to publication, including the timing of publication, with respect to intellectual property. In so doing we confirm that we have followed the regulations of our institutions concerning intellectual property.

Declaration of competing interest

The authors declare that they have no known competing financial interests or personal relationships that could have appeared to influence the work reported in this paper.

Acknowledgements

Centre for Instrumentation Sharing – University of Pisa (CISUP) is thanked for its support in the use of FEI Quanta 450 FEG scanning electron microscope.

References

[1] R. Narayan, Drivers and Rationale for use of biobased materials based on life cycle assessment (LCA), in: Glob. Plast. Environ. Conf. Atlanta, 2004.
[2] F.P. La Mantia, M. Morreale, L. Botta, M.C. Mistretta, M. Ceraulo, R. Scaffaro, Degradation of polymer blends: a brief review, Polym. Degrad. Stabil. 145 (2017) 79–92, https://doi.org/10.1016/j.polymdegradstab.2017.07.011.
[3] M. Coltelli, L. Aliotta, V. Gigante, M. Bellusci, P. Cinelli, E. Bugnicourt, M. Schmid, A. Staebler, A. Lazzeri, Preparation and compatibilization of PBS/whey protein isolate based blends, Molecules 25 (2020) 1–15, https://doi.org/10.3390/molecules25143313.
[4] P. Cinelli, M. Seggiani, N. Mallegni, V. Gigante, A. Lazzeri, Processability and degradability of PHA-based composites in terrestrial environments, Int. J. Mol. Sci. 20 (2019), https://doi.org/10.3390/ijms20020284.
[5] U. Sonchaeng, F. Iniguez-Franco, R. Auras, S. Selke, M. Rubino, L.-T. Lim, Poly (lactic acid) mass transfer properties, Prog. Polym. Sci. 86 (2018) 85–121.
[6] L.T. Lim, R. Auras, M. Rubino, Processing technologies for poly(lactic acid), Prog. Polym. Sci. 33 (2008) 820–852, https://doi.org/10.1016/j.progpolymsci.2008.05.004.
[7] D. Garlotta, A literature review of poly (lactic acid), J. Polym. Environ. 9 (2001) 63–84.
[8] L. Aliotta, M. Gazzano, A. Lazzeri, M.C. Righetti, Constrained amorphous interphase in poly (L -lactic acid): estimation of the tensile elastic modulus, ACS Omega 5 (2020) 20890–20902, https://doi.org/10.1021/acsomega.0c02330.
[9] K.K.S. Anderson, K.K.M. Schreck, M.A. Hillmyer, Toughening polylactide, Polym. Rev. 48 (2008) 85–108, https://doi.org/10.1080/15583720701834216.
[10] L. Aliotta, V. Gigante, M. Coltelli, P. Cinelli, A. Lazzeri, M. Seggiani, Thermo-mechanical properties of PLA/short flax fiber biocomposites, Appl. Sci. 9 (2019) 1–15, https://doi.org/10.3390/app9183797.
[11] J.M. Raquez, Y. Habibi, M. Murariu, P. Dubois, Polylactide (PLA)-based nanocomposites, Prog. Polym. Sci. 38 (2013) 1504–1542, https://doi.org/10.1016/j.progpolymsci.2013.05.014.
[12] V. Gigante, I. Canesi, P. Cinelli, M.B. Coltelli, A. Lazzeri, Rubber toughening of polylactic acid (PLA) with poly(butylene adipate-co-terephthalate) (PBAT): mechanical properties, fracture mechanics and analysis of ductile-to-brittle behavior while varying temperature and test speed, Eur. Polym. J. 115 (2019) 125–137, https://doi.org/10.1016/j.eurpolymj.2019.03.015.
[13] K. Zhang, V. Nagarajan, M. Misra, A.K. Mohanty, Supertoughened renewable PLA reactive multiphase blends system: phase morphology and performance, ACS Appl. Mater. Interfaces 6 (2014) 12436–12448.

[14] L. Aliotta, A. Vannozzi, L. Panariello, V. Gigante, M.B. Coltelli, A. Lazzeri, Sustainable micro and nano additives for controlling the migration of a biobased plasticizer from PLA - based flexible films, Polymers 12 (2020) 1–25, https://doi.org/10.3390/polym12061366.

[15] T. Mekonnen, P. Mussone, H. Khalil, D. Bressler, Progress in bio-based plastics and plasticizing modifications, J. Mater. Chem. A. 1 (2013) 13379–13398, https://doi.org/10.1039/c3ta12555f.

[16] O. Martin, L. Avérous, Poly(lactic acid): plasticization and properties of biodegradable multiphase systems, Polymer 42 (2001) 6209–6219, https://doi.org/10.1016/S0032-3861(01)00086-6.

[17] M. Shibata, Y. Someya, M. Orihara, M. Miyoshi, Thermal and mechanical properties of plasticized poly (l-lactide) nanocomposites with organo-modified montmorillonites, J. Appl. Polym. Sci. 99 (2006) 2594–2602.

[18] J.F. Zhang, X. Sun, Physical characterization of coupled poly(lactic acid)/starch/maleic anhydride blends plasticized by acetyl triethyl citrate, Macromol. Biosci. 4 (2004) 1053–1060, https://doi.org/10.1002/mabi.200400076.

[19] L.V. Labrecque, R.A. Kumar, V. Davé, R.A. Gross, S.P. Mccarthy, Citrate esters as plasticizers for poly(lactic acid), J. Appl. Polym. Sci. 66 (1997) 1507–1513, https://doi.org/10.1002/(SICI)1097-4628(19971121)66:8<1507::AID-APP11>3.0.CO;2-0.

[20] M. Maiza, M.T. Benaniba, V. Massardier-Nageotte, Plasticizing effects of citrate esters on properties of poly(lactic acid), J. Polym. Eng. 36 (2016) 371–380, https://doi.org/10.1515/polyeng-2015-0140.

[21] L. Aliotta, P. Cinelli, M. Beatrice Coltelli, A. Lazzeri, Rigid filler toughening in PLA-Calcium Carbonate composites: effect of particle surface treatment and matrix plasticization, Eur. Polym. J. (2018), https://doi.org/10.1016/j.eurpolymj.2018.12.042.

[22] M.B. Coltelli, I. Della Maggiore, M. Bertoldo, F. Signori, S. Bronco, F. Ciardelli, Poly (lactic acid) properties as a consequence of poly(butylene adipate-co-terephthalate) blending and acetyl tributyl citrate plasticization, J. Appl. Polym. Sci. 110 (2008) 1250–1262, https://doi.org/10.1002/app.28512.

[23] C. Courgneau, V. Ducruet, L. Avérous, J. Grenet, S. Domenek, Nonisothermal crystallization kinetics of poly (lactide)—effect of plasticizers and nucleating agent, Polym. Eng. Sci. 53 (2013) 1085–1098.

[24] H. Liu, J. Zhang, Research progress in toughening modification of poly (lactic acid), J. Polym. Sci., Part B: Polym. Phys. 49 (2011) 1051–1083.

[25] J. Urquijo, G. Guerrica-Echevarría, J.I. Eguiazábal, Melt processed PLA/PCL blends: effect of processing method on phase structure, morphology, and mechanical properties, J. Appl. Polym. Sci. 132 (2015).

[26] S. Kuo, C. Huang, Y. Tung, F. Chang, Effect of bisphenol A on the miscibility, phase morphology, and specific interaction in immiscible biodegradable poly (ε-caprolactone)/poly (l-lactide) blends, J. Appl. Polym. Sci. 100 (2006) 1146–1161.

[27] T. Semba, K. Kitagawa, U.S. Ishiaku, H. Hamada, The effect of crosslinking on the mechanical properties of polylactic acid/polycaprolactone blends, J. Appl. Polym. Sci. 101 (2006) 1816–1825, https://doi.org/10.1002/app.23589.

[28] M. Todo, T. Takayama, Fracture mechanisms of biodegradable PLA and PLA/PCL blends, Biomater. Chem. (2011).

[29] A. Bhatia, R.K. Gupta, S.N. Bhattacharya, H.J. Choi, Compatibility of biodegradable poly (lactic acid) (PLA) and poly (butylene succinate) (PBS) blends for packaging application, Korea Aust. Rheol. J. 19 (2007) 125–131, https://doi.org/10.1155/2010/287082.

[30] M. Shibata, Y. Inoue, M. Miyoshi, Mechanical properties, morphology, and crystallization behavior of blends of poly (L-lactide) with poly (butylene succinate-co-L-lactate) and poly (butylene succinate), Polymer 47 (2006) 3557–3564.

[31] J.W. Park, S.S. Im, Phase behavior and morphology in blends of poly (L-lactic acid) and poly (butylene succinate), J. Appl. Polym. Sci. 86 (2002) 647–655.

[32] S. Lee, J.W. Lee, Characterization and processing of Biodegradable polymer blends of poly(lactic acid) with poly(butylene succinate adipate), Korea, Aust. Rheol. J. 17 (2005) 71–77.

[33] V. Ojijo, S. Sinha Ray, R. Sadiku, Role of specific interfacial area in controlling properties of immiscible blends of biodegradable polylactide and poly [(butylene succinate)-co-adipate], ACS Appl. Mater. Interfaces 4 (2012) 6690–6701.

[34] S.A. Pradeep, H. Kharbas, L.S. Turng, A. Avalos, J.G. Lawrence, S. Pilla, Investigation of thermal and thermomechanical properties of biodegradable PLA/PBSA composites processed via supercritical fluid-assisted foam injection molding, Polymers (2017) 9, https://doi.org/10.3390/polym9010022.

[35] M.A. Abdelwahab, A. Flynn, B. Sen Chiou, S. Imam, W. Orts, E. Chiellini, Thermal, mechanical and morphological characterization of plasticized PLA-PHB blends, Polym. Degrad. Stabil. 97 (2012) 1822–1828, https://doi.org/10.1016/j.polymdegradstab.2012.05.036.

[36] M.P. Arrieta, M.D. Samper, M. Aldas, J. López, On the use of PLA-PHB blends for sustainable food packaging applications, Materials 10 (2017) 1–26, https://doi.org/10.3390/ma10091008.

[37] M.P. Arrieta, E. Fortunati, F. Dominici, J. López, J.M. Kenny, Bionanocomposite films based on plasticized PLA–PHB/cellulose nanocrystal blends, Carbohydr. Polym. 121 (2015) 265–275, https://doi.org/10.1016/j.carbpol.2014.12.056.

[38] M. Nofar, A. Maani, H. Sojoudi, M.C. Heuzey, P.J. Carreau, Interfacial and rheological properties of PLA/PBAT and PLA/PBSA blends and their morphological stability under shear flow, J. Rheol. 59 (2015) 317–333, https://doi.org/10.1122/1.4905714.

[39] M. Nishida, H. Ichihara, H. Watanabe, N. Fukuda, H. Ito, Improvement of dynamic tensile properties of Poly(lactic acid)/Poly(butylene adipate-co-terephthalate) polymer alloys using a crosslinking agent and observation of fracture surfaces, Int. J. Impact Eng. 79 (2015) 117–125, https://doi.org/10.1016/j.ijimpeng.2014.11.010.

[40] L. Botta, M.C. Mistretta, S. Palermo, M. Fragalà, F. Pappalardo, Characterization and processability of blends of polylactide acid with a new biodegradable medium-chain-length polyhydroxyalkanoate, J. Polym. Environ. 23 (2015) 478–486, https://doi.org/10.1007/s10924-015-0729-4.

[41] M. Nofar, M.C. Heuzey, P.J. Carreau, M.R. Kamal, J. Randall, Coalescence in PLA-PBAT blends under shear flow: effects of blend preparation and PLA molecular weight, J. Rheol. 60 (2016) 637–648, https://doi.org/10.1122/1.4953446.

[42] S.Y. Gu, K. Zhang, J. Ren, H. Zhan, Melt rheology of polylactide/poly(butylene adipate-co-terephthalate) blends, Carbohydr. Polym. 74 (2008) 79–85, https://doi.org/10.1016/j.carbpol.2008.01.017.

[43] K. Hamad, M. Kaseem, M. Ayyoob, J. Joo, F. Deri, Polylactic acid blends: the future of green, light and tough, Prog. Polym. Sci. 85 (2018) 83–127, https://doi.org/10.1016/j.progpolymsci.2018.07.001.

[44] L. Jiang, M.P. Wolcott, J. Zhang, Study of biodegradable polylactide/poly(butylene adipate-co-terephthalate) blends, Biomacromolecules 7 (2006) 199–207, https://doi.org/10.1021/bm050581q.

[45] L. Aliotta, V. Gigante, O. Acucella, F. Signori, A. Lazzeri, Thermal, Mechanical and Micromechanical Analysis of PLA/PBAT/POE-g-GMA Extruded Ternary Blends, (n. d.).

[46] M. Kumar, S. Mohanty, S.K. Nayak, M. Rahail Parvaiz, Effect of glycidyl methacrylate (GMA) on the thermal, mechanical and morphological property of biodegradable PLA/PBAT blend and its nanocomposites, Bioresour. Technol. 101 (2010) 8406–8415, https://doi.org/10.1016/j.biortech.2010.05.075.

[47] V. Mishra, F.E. Du Prez, E.J. Goethals, L.H. Sperling, Simultaneous interpenetrating networks of a polyurethane and poly(methyl methacrylate). II. Partitioning of MMA monomer in the last stages of polymerization, J. Appl. Polym. Sci. 58 (1995) 347–356, https://doi.org/10.1002/app.1995.070580214.

[48] J. Ma, R.M. Larsen, Comparative study on dispersion and interfacial properties of single walled carbon nanotube/polymer composites using hansen solubility parameters, ACS Appl. Mater. Interfaces 5 (2013) 1287–1293, https://doi.org/10.1021/am302407z.

[49] C.M. Hansen, Hansen Solubility Parameters:a User's Handbook, second ed., CRC press, New York, 2000.

[50] J.M. Pochan, C.L. Beatty, D.F. Pochan, Different approach for the correlation of the Tg of mixed amorphous systems, Polymer 20 (1979) 879–886, https://doi.org/10.1016/0032-3861(79)90128-9.

[51] T.G. Fox, Influence of diluent and of copolymer composition on the glass temperature of a poly-mer system, Bull. Am. Phys. Soc. 1 (1956) 123.

[52] M.C. Shen, A. V Tobolsky, Plasticization and plasticizer processes, Adv. Chem. 48 (1965) 27.

[53] M. Gordon, J.S. Taylor, Ideal copolymers and the second-order transitions of synthetic rubbers. I. Non-crystalline copolymers, J. Appl. Chem. 2 (1952) 493–500.

[54] J. V Koleske, R.D. Lundberg, Lactone polymers. I. Glass transition temperature of poly-ε-caprolactone by means on compatible polymer mixtures, J. Polym. Sci. 2 Polym. Phys. 7 (1969) 795–807.

[55] H. Fujita, A. Kishimoto, Diffusion-controlled stress relaxation in polymers. II. Stress relaxation in swollen polymers, J. Polym. Sci. 28 (1958) 547–567.

[56] R.F. Boyer, R.S. Spencer, Effect of plasticizers on second-order transition points of high polymers, J. Polym. Sci. 2 (1947) 157–177.

[57] W. Kauzmann, H. Eyring, The viscous flow of large molecules, J. Am. Chem. Soc. 62 (1940) 3113–3125.

[58] C.M. Hansen, A.L. Smith, Using Hansen solubility parameters to correlate solubility of C60 fullerene in organic solvents and in polymers, Carbon N. Y. 42 (2004) 1591–1597.

[59] D.P. Faasen, A. Jarray, H.J.W. Zandvliet, E.S. Kooij, W. Kwiecinski, Hansen solubility parameters obtained via molecular dynamics simulations as a route to predict siloxane surfactant adsorption, J. Colloid Interface Sci. (2020).

[60] A. Alghunaim, S. Kirdponpattara, B.Z. Newby, Techniques for determining contact angle and wettability of powders, Powder Technol. 287 (2016) 201–215.

[61] L. Fang, R. Singh, L. Waxman, C. Zhao, Model protein adsorption on polymers explained by hansen solubility parameters, J. Pharm. Sci. 108 (2019) 187–192.

[62] R. Auras, L.-T. Lim, S.E.M. Selke, H. Tsuji, eds., Poly(lactic acid): Synthesis, Structures, Properties, Processing, and Applications, John Wiley & Sons, Inc., 210AD.

[63] C.M. Hansen, The universality of the solubility parameter, Ind. Eng. Chem. Prod. Res. Dev. 8 (1969) 2–11.

[64] G.C. Vebber, P. Pranke, C.N. Pereira, Calculating hansen solubility parameters of polymers with genetic algorithms, J. Appl. Polym. Sci. 131 (2014) 1–12, https://doi.org/10.1002/app.39696.

[65] A. Ruellan, A. Guinault, C. Sollogoub, V. Ducruet, S. Domenek, Solubility factors as screenin tools of biodegrdable toughneing agents of polylactide, J. Appl. Polym. Sci. 132 (2015) 1–11, https://doi.org/10.1002/app.42476.

[66] G. Jing, USING HANSEN SOLUBILITY PARAMETERS (HSPS) TO DEVELOP ANTIOXIDANT-PACKAGING FILM TO ACHIEVE CONTROLLED RELEASE, Michigan State University, 2014.

[67] M. Răpă, R.N. Darie-Niță, E. Grosu, E.E. Tănase, A.R. Trifoi, T. PAPa, C. Vasile, Effect of plasticizers on melt processability and properties of PHB, J. Optoelectron. Adv. Mater. 17 (2015) 1778–1784.

[68] D. Sauer, J.W. McGinity, Influence of additives on melt viscosity, surface tension, and film formation of dry powder coatings, Drug Dev. Ind. Pharm. 35 (2009) 646–654.

[69] C. Courgneau, S. Domenek, A. Guinault, L. Avérous, V. Ducruet, Analysis of the structure-properties relationships of different multiphase systems based on plasticized poly(lactic acid), J. Polym. Environ. 19 (2011) 362–371, https://doi.org/10.1007/s10924-011-0285-5.

[70] S.K. Nayak, Biodegradable PBAT/Starch nanocomposites, Polym. Plast. Technol. Eng. 49 (2010) 1406–1418, https://doi.org/10.1080/03602559.2010.496397.
[71] E.W. Fischer, H.J. Sterzel, G. Wegner, Investigation of the structure of solution grown crystals of lactide copolymers by means of chemical reactions, Kolloid-Z. Z. Polym. 251 (1973) 980–990, https://doi.org/10.1007/BF01498927.
[72] L.C. Arruda, M. Magaton, R.E.S. Bretas, M.M. Ueki, Influence of chain extender on mechanical, thermal and morphological properties of blown films of PLA/PBAT blends, Polym. Test. (2015), https://doi.org/10.1016/j.polymertesting.2015.02.005.
[73] E. Quero, A.J. Müller, F. Signori, M.B. Coltelli, S. Bronco, Isothermal cold-crystallization of PLA/PBAT blends with and without the addition of acetyl tributyl citrate, Macromol. Chem. Phys. 213 (2012) 36–48, https://doi.org/10.1002/macp.201100437.
[74] R. Al-Itry, K. Lamnawar, A. Maazouz, N. Billon, C. Combeaud, Effect of the simultaneous biaxial stretching on the structural and mechanical properties of PLA, PBAT and their blends at rubbery state, Eur. Polym. J. (2015), https://doi.org/10.1016/j.eurpolymj.2015.05.001.
[75] P. Hongdilokkul, K. Keeratipinit, S. Chawthai, B. Hararak, M. Seadan, S. Suttiruengwong, A study on properties of PLA/PBAT from blown film process, IOP Conf. Ser. Mater. Sci. Eng. 87 (2015), https://doi.org/10.1088/1757-899X/87/1/012112.
[76] A. Lazzeri, C.B. Bucknall, Dilatational bands in rubber-toughened polymers, J. Mater. Sci. 28 (1993) 6799–6808, https://doi.org/10.1007/BF00356433.
[77] A. Lazzeri, C.B. Bucknall, Recent developments in the modeling of dilatational yielding in toughened plastics, Toughening Plast, Adv. Model. Exp. (2000) 264.
[78] M. Maiza, M.T. Benaniba, G. Quintard, V. Massardier-Nageotte, Biobased additive plasticizing Polylactic acid (PLA), Polimeros 25 (2015) 581–590, https://doi.org/10.1590/0104-1428.1986.
[79] I. Pillin, N. Montrelay, Y. Grohens, Thermo-mechanical characterization of plasticized PLA: is the miscibility the only significant factor? Polymer 47 (2006) 4676–4682, https://doi.org/10.1016/j.polymer.2006.04.013.
[80] N. Mallegni, T.V. Phuong, M.B. Coltelli, P. Cinelli, A. Lazzeri, Poly(lactic acid) (PLA) based tear resistant and biodegradable flexible films by blown film extrusion, Materials 11 (2018), https://doi.org/10.3390/ma11010148.
[81] Z. Gan, K. Kuwabara, M. Yamamoto, H. Abe, Y. Doi, Solid-state structures and thermal properties of aliphatic–aromatic poly (butylene adipate-co-butylene terephthalate) copolyesters, Polym. Degrad. Stabil. 83 (2004) 289–300.
[82] C. Harrats, G. Groeninckx, Reactive processing of polymer blend using reactive compatibilization and dynamic crosslinking: phase morphology control and microstructure–property relations, in: Modif. Blending Synth. Nat. Macromol., Springer, 2004, pp. 155–199.
[83] J.J. Elmendorp, A study on polymer blending microrheology, Polym. Eng. Sci. 26 (1986) 418–426.